ChemComm

Room temperature formation of rhodium nanoparticles on TiO_2[110] *via* MetalOrganic Chemical-Vapour Deposition (MOCVD) of $[Rh(CO)_2Cl]_2$

Mark A. Newton,*[a] Roger A. Bennett,*[b] Rupert D. Smith,[b] Michael Bowker[b] and John Evans[a]

[a] *Department of Chemistry, University of Southampton, Highfield, Southampton, UK SO17 1BJ. E-mail: m.a.newton@soton.ac.uk*

[b] *Centre for Surface Science and Catalysis, Department of Chemistry, University of Reading, Whiteknights Park, Reading, UK RG6 6AD. E-mail: r.a.bennett@reading.ac.uk*

Received (in Cambridge, UK) 11th May 2000, Accepted 25th July 2000

Room temperature adsorption of $[Rh(CO)_2Cl]_2$ on TiO_2[110] is investigated using Scanning Tunnelling Microscopy (STM) which reveals the formation of nanoparticles that coexist with the mono-disperse $Rh(CO)_2Cl$ species; the spatial distribution of these particles indicates that nanoparticle formation occurs principally at step edges.

Since the determination of the existence of mono-disperse $Rh^I(CO)_2$ species on supported Rh systems[1] a wealth of research has been directed at quantifying the role played by this species in Rh based catalysts, particularly with regards to NO_x removal processes.[2–9] CO may also oxidatively disrupt small metallic Rh clusters forming $Rh^I(CO)_2$.[10–13] A complete understanding of the behaviour of supported Rh systems must therefore include a detailed knowledge of how this species behaves under a variety of conditions.

Model supported $Rh^I(CO)_2$ systems can be created *via* two routes. Firstly, catalysts may be prepared from $RhCl_3$ which, after calcination and reduction, may be redispersed using CO to give an adsorbed layer of $Rh(CO)_2$ species.[1,7,14] Typically, however, this method is only viable for Rh loadings of < 2.5 wt%. A second approach is to use a volatile Rh organometallic which may be adsorbed to a prepared oxide surface to yield a $Rh(CO)_2$ adlayer directly.[15–17] As the $Rh^I(CO)_2$ is immediately present it has the perceived advantage of accessing higher Rh loadings whilst still producing a truly mono-disperse adlayer. The use of MetalOrganic Chemical-Vapour Deposition (MOCVD) of Rh organometallics has found particular favour in surface science studies of the chemistry of $Rh^I(CO)_2$ species[17] adsorbed on single crystal oxide surfaces. In these cases involatile inorganic salts, such as $RhCl_3$ may not be used, and the larger Rh clusters formed by Metal Vapour Deposition (MVD) may not be re-dispersed to yield a mono-disperse $Rh^I(CO)_2$ adlayer.[17]

Previous studies concerning the adsorption of $[Rh(CO)_2Cl]_2$ on both high area and [110] oriented single crystal rutile, have indicated that the dissociative adsorption of this species results in a uniform $Rh^I(CO)_2Cl$ adlayer.[15–17] However, there has been no determination of the local structures that result from the adsorption as no LEED structures[17] have been observed. Evidence for a molecular orientation with Rh–C–O bonds aligned in the $< 1\bar{1}0 >$ azimuth has however been demonstrated by Fourier Transform Reflection Absorption Infrared Spectroscopy.[18] We have therefore employed Scanning Tunnelling Microscopy (STM) to determine how the adsorbed $Rh^I(CO)_2Cl$ species interact with the surface and each other.

Experiments were carried out in a UHV chamber equipped with LEED/Auger, and variable temperature STM facilities.[19] The preparation of the rutile TiO_2[110](1 × 1)[20] surface, and the purification of the organometallic sample[17] have been described previously. Rh dosing was controlled *via* a fine leak valve and a line of sight tube doser permitting *in situ* STM measurements whilst the surface is being exposed the organometallic vapour. Unfortunately adsorption of carbonyl along the length of the tube precludes a sharp transition between 'on' and 'off' so considerable exposure of the surface continues after shutting the valve. All STM measurements were carried out with a positive sample bias and therefore unoccupied electronic states are imaged.

Fig. 1(*a*) shows a (97 × 97 Å) STM image of a freshly deposited $Rh(CO)_2Cl$ adlayer. The layer consists of elements showing some low level of local order. The average area per individual unit in Fig 1(*a*) is 40–50 Å^2 which places the coverage at *ca.* 0.2 ML where 1 ML is equivalent to the density of Ti in the surface (0.1 Ti Å^{-2}). Comparison of images taken before and after dosing indicate the features reside preferentially near the centre of the dark rows imaged on the clean TiO_2; *i.e.* on the rows of bridging oxygen. Lack of resolution precludes determination of the lateral position along the row.

Fig. 1(*b*) shows an area (198 × 198 Å) of the same adlayer *ca.* 40 minutes after initial deposition. The features now show a distinct ordering with the appearance of rows on the surface running in two rotationally related domains at ±42 ± 3° to the principal crystallographic directions. The apparent density of the species has increased within this more ordered adlayer and each feature now occupies 25–30 Å^2 corresponding to *ca.* 0.35–0.4 ML. This increased density is due to continued exposure from the dosing tube as mentioned above, and represents a saturation coverage of $Rh(CO)_2Cl$. Given the tunnelling conditions used (above), the size and density of the small features observed in Figs. 1(*a*) and (*b*), we associate these with the $4d_{x^2-y^2}$) orbital of individual, square planar coordinated Rh^I atoms. We believe that the Cl is intimately associated with the $Rh(CO)_2$ and not adsorbed as a separate species. Cl adsorbed upon TiO_2[110][21] appears as an anomalously large (*ca.* 6–8 Å diameter), immobile bright feature in STM: the features we observe do not show such character.

The adlayer in Fig 1(*b*) does show a LEED pattern. However, it is destroyed within *ca.* 2 seconds exposure to the LEED electron beam; the details of this structure will be discussed in a future communication. Also visible in Fig. 1(*b*) are two new

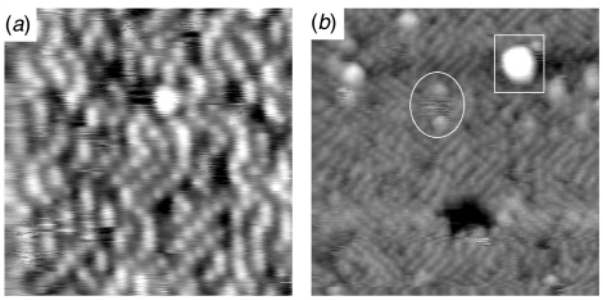

Fig. 1 (*a*) STM image (97 × 97 Å, 1 V, 0.3 nA) of a freshly prepared adlayer derived from room temperature adsorption of $[Rh(CO)_2Cl]_2$ to the TiO_2[110](1 × 1) surface approximately 3 minutes after dosing. (*b*) STM image (198 × 198 Å, 1 V, 0.3 nA) of the adlayer shown in Fig. 1(*a*) approximately 40 minutes after dosing. A large discrete particle is marked by the rectangle while an oval marks two of the smaller, less distinct, particles.

DOI: 10.1039/b003782f

types of feature: the first comprises small, indistinct particles with an apparent height slightly greater than the $Rh(CO)_2Cl$ adlayer; the second comprises discrete larger particles.

Fig. 2 shows a large area scan (998 × 998 Å) of the surface approximately 150 minutes after deposition. The large particles shown in Fig. 1(*b*) are found all over the surface preferentially residing at step edges of the underlying rutile. The particles co-exist with the $Rh(CO)_2Cl$ adlayer. Taking the width of the step region to be that of the largest particle we find large particle formation in the step region to be 5 times more probable than on the terrace on an area for area basis. This indicates that a regio-specific formation of Rh nanoparticles occurs alongside the production of domains of $Rh^I(CO)_2Cl$. Smaller particles are also observed but do not show a distribution that favours the step edges. This particulate formation is not an artefact due to the presence of the tip; moving the tip to new areas of the surface yields similar images.

Fig. 3 shows the particle size distributions derived from Fig. 2 in terms of particle heights, areas, volumes and perimeters. The distributions show two clear groups; a multitude of small particles, and long tail of large particles. An analysis of the height and volume data for the larger particles indicates that they contain up to a few hundred atoms at maximum. The total volume of these particles is *ca*. 435000 Å^3 giving an effective coverage of *ca*. 0.3 ML Rh in particulate form (assuming a bulk Rh lattice constant). It should also be noted, however, that

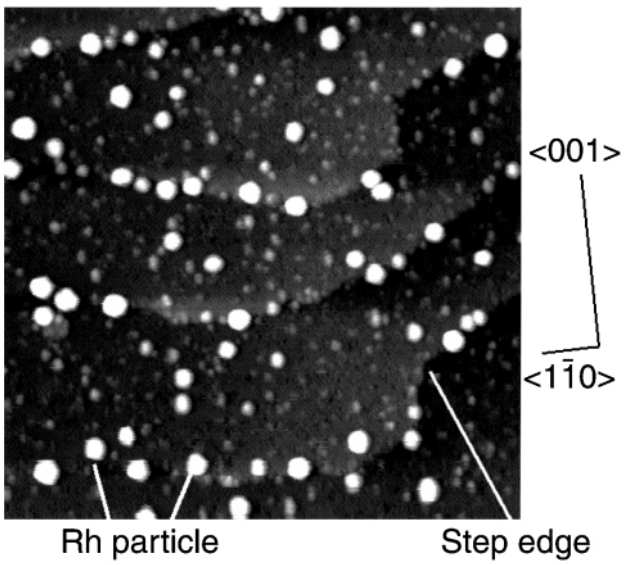

Fig. 2 Large area STM image (998 × 998 Å, 1 V, 0.1 nA) taken *ca*. 150 minutes after Rh deposition.

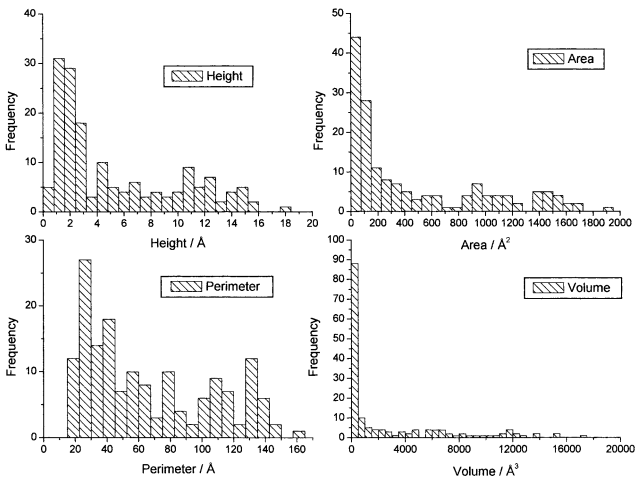

Fig. 3 Particle size distribution functions for Fig. 2. Area and perimeter are derived directly from the particles projected shape onto the surface, while volume and height are calculated from the apparent height and therefore may be influenced by electronic effects.

preliminary analysis of the scaling relationships of the measured parameters of Fig. 2 (*i.e.* volume, area, height *versus* perimeter) indicates that the particles have a well-defined shape despite the apparent lack of clear facets.

The spatial distribution of these particles is distinct from similar Rh particles grown *via* MVD which are reported to show no preferential decoration of step edges.[22] The reasons for this are as yet unclear, but this most probably relates to the need to activate the decomposition of the carbonyl in MOCVD, *versus* the surface diffusion limited growth in MVD.

In summary, and in contrast to a number of previous investigations,[15–17] we have shown that room temperature MOCVD of $[Rh(CO)_2Cl]_2$ does not necessarily lead to a uniform mono-disperse $Rh(CO)_2Cl$ adlayer. Adsorption of this species may initially result in formation of such a layer but this configuration is only metastable even at room temperature. Room temperature adsorption of $[Rh(CO)_2Cl]_2$ on vacuum reduced TiO_2[110] can result in the formation of Rh nano-particles that are distinct from similar sized particles grown *via* MVD, and that may coexist with an ordered layer of $Rh^I(CO)_2Cl$ species. The spatial distribution of these particles indicates that step edges on the rutile surface act as enhanced sites for nucleation of particulate Rh *via* the decomposition of the $Rh(CO)_2Cl$ species. Terraces show a much lower rate of particle formation. We have therefore demonstrated a previously unknown chemistry of TiO_2[110] step edges that produces the nanoparticles. Further, our results indicate that, in systems such as this, the time-scale of interrogation must be considered due to the possibility of changes in the phase of the adsorbed metal species.

We thank the EPSRC for post-doctoral funding to M. A. N. and R. A. B., and the EPSRC/Johnson Matthey PLC for funding a CASE award to R. D. S. We also thank A. J. Ramirez-Cuesta for development of the particle analysis software.

Notes and references

1 A. C. Yang and C. W. Garland, *J. Phys. Chem.*, 1957, **61**, 1504.
2 H. Arai and H. Tominanga, *J. Catal.*, 1976, **43**, 131.
3 G. Srinvas, S. S. C. Chuang and S. Debnath, *J. Catal.*, 1994, **148**, 748.
4 E. A. Hyde and R. Rudham, *J. Chem. Soc., Faraday Trans.*, 1984, **80**, 531.
5 R. Krishnamurthy and S. S. C. Chuang, *J. Phys. Chem.*, 1995, **99**, 16 727.
6 S. H. Oh and C. Eickel, *J. Catal.*, 1991, **128**, 526.
7 K. Almusaiteer, S. S. C. Chuang and C. D. Tan, *J Catal.*, 2000, **189**, 247.
8 T. Chafik, D. I. Kondarides and X. E. Verykios, *J. Catal.*, 2000, **190**, 446; D. I. Kondarides, T. Chafik and X. E. Verykios, *J. Catal.*, 2000, **191**, 147.
9 H. F. T. Van't Blik, J. B. A. D. van Zon, T. Huizinga, J. C. Vis, D. C. Koningsberger and R. Prins, *J Phys. Chem.*, 1983, **87**, 2264.
10 S. S. C. Chuang and C. D. Tan, *J. Catal.*, 1988, **173**, 95.
11 P. Johnston and R. W. Joyner, *J. Chem. Soc., Faraday Trans.*, 1993, **89**, 863.
12 P. Johnston, R. W. Joyner, P. D. A. Pudney, E. S. Shpiro and B. P. Williams, *Faraday Discuss. Chem. Soc.*, 1990, **89**, 144.
13 F. Solymosi, T. Bansagi and E. Novak, *J. Catal.*, 1988, **112**, 183.
14 For example: J. T. Yates, T. M. Duncan, S. D. Worley and R. W. J. Vaughan, *J. Chem. Phys.*, 1979, **71**, 1219.
15 M. P. Keyes and K. L. Watters, *J. Catal.*, 1986, **100**, 44; *J. Catal.*, 1988, **100**, 96.
16 B. G. Frederick, G. Apai and T. N. Rhodin, *J. Am. Chem. Soc.*, 1987, **109**, 4797.
17 J. Evans, B. E. Hayden, F. Mosselmans and A. Murray, *J. Am. Chem. Soc.*, 1992, **114**, 6912; J. Evans, B. E. Hayden, F. Mosselmans and A. Murray, *Surf. Sci.*, 1994, **301**, 61.
18 B. E. Hayden, A. King and M. A. Newton, *Chem. Phys. Lett.*, 1997, **269**, 485.
19 M. Bowker, S. Poulston, R. A. Bennett, P. Stone, A. H. Jones, S. Haq and P. Hollins, *J. Mol. Catal. A: Chemical*, 1998, **131**, 185.
20 R. A. Bennett, P. Stone and M. Bowker, *Faraday Discuss.*, 1999, **114**, 267.
21 U. Diebold, W. Hebenstreit, G. Leonardi, M. Schmid and P. Varga, *Phys. Rev. Lett.*, 1998, **81**, 405.
22 A. Berkó, G. Ménesi and F. Solymosi, *Surf. Sci.*, 1997, **372**, 202.